Fabrication of fibre-Bragg-gratings in various high birefringent optical fibres for advanced FBG sensing applications

F. Jülich [1)], A.W. Koch [2)] and J. Roths [1)]
[1)] Hochschule München, Lothstr. 34, 80335 München
[2)] TU München, Theresienstr. 90, 80333 München

Introduction

In 1978, K.O. Hill discovered a permanent change of the refractive index of a Germanium doped optical fibre when exposed to ultraviolet light. This effect, the so-called photosensitivity has been used by Hill and co workers[1] for the inscription of Bragg-gratings into optical fibres. Since this investigation, the formation of fibre-Bragg-gratings (FBG) has been demonstrated in a large variety of different types of optical fibres. The optical properties of a FBG are correlated to the type of fibre as well as the mechanical and thermal load applied to the optical fibre. Therefore, FBGs have become a new type of sensor for strain, temperature and multi-parameter[2] sensing. With spreading of the fibre-Bragg-grating based sensor technology, there is also a growing demand on high accurate sensors.

Standard fibre Bragg grating sensors (FBGS) are typically inscribed into single mode optical fibres (SMF). Due to the optical properties of these fibres, standard FBGS show a dependence of their Bragg reflection wavelength λ_B on the state of polarization (SOP) of the light waves that interact with the FBG. The dependence of λ_B on the SOP of the light wave is due to a certain amount of birefringence present in the optical fibre at the location of the FBG. The origin of this birefringence is from both, the residual birefringence of the pristine fibre and the birefringence that was induced during the inscription process.

When standard FBGS are used for sensing, these variations of λ_B may result in uncertainties of the measurement. With this type of FBG we measured variations of λ_B in the range of ~5pm to ~20pm as a function of the input SOP, see Figure 1. The typical temperature sensitivity of FBGs of ~10pm/℃ resul ts in uncertainties of 0.5℃ – 2.0℃ for temperature s ensing. When standard FBGS are used for strain sensing, the variations of λ_B are equivalent to 4µm/m – 16µm/m mechanical strain. This limits the accuracy of standard fibre-Bragg-grating Sensors.

Since it is difficult to produce FBGs with ultra-low birefringence in a reproducible way, our intention is to employ FBGs that were inscribed into highly birefringent or polarisation maintaining optical fibres[3]. A FBG under high birefringence is characterised by the spectral separation of the Bragg-reflection peak into two separated peaks. While standard single mode fibres are not capable of maintaining the input state of polarisation (SOP) for more than a few meters[4], highly birefringent fibres (HiBi-fibres) maintain the SOP and therefore, interrogation of FBGs with a controlled SOP is possible in HiBi-fibres.

In this study, we inscribed FBGs in various types of highly birefringent fibres. By measuring the Bragg-wavelengths of the separated reflection peaks during the inscription process, we were able to determine the effective refractive indices for both optical axis and the magnitude of the birefringence of the pristine fibre.

Theory

An optical fibre Bragg-grating bases upon a permanent, periodic variation of the refractive index within the core of an optical fibre[5]. These structures are generated by the exposure of the photosensitive (GeO_2) doped core of optical fibres to a UV interference pattern. The phase mask technique[6] employed in this study generates an interference pattern, whose period Λ is directly related to the grating period of the phase mask Λ_{PM}, by

$$\Lambda = \frac{\Lambda_{PM}}{2}. \quad (1)$$

A periodic variation of the refractive index, with an amplitude Δn and pitch Λ is generated over a length L inside the core of the fibre by exposure to the UV pattern. The change of the refractive index along the region of the fibre may be divided into an alternating (approximate sinusoidal) variation of the refractive index (Δn_{AC}) and an offset (Δn_{DC}), see Figure 2. The effective refractive index n_{eff} of a fibre that is exposed to a certain amount of UV light can be approximately described as a function of the UV dose (*d*),

$$n_{eff}(d) = n_{eff} + \left(\Delta n_{\mathrm{DC}}(d) + \Delta n_{\mathrm{AC}}(d)\right). \quad (2)$$

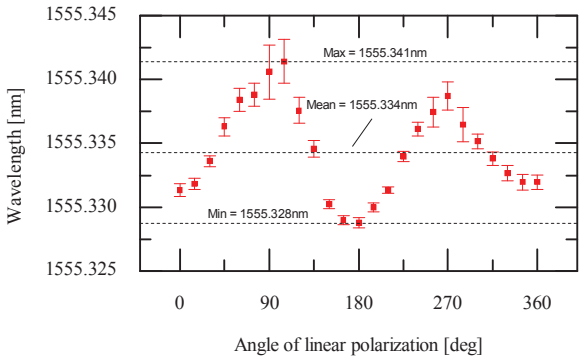

Figure 1: Wavelength dependence of a SM-FBG to the angle of the plane of linear polarisation.

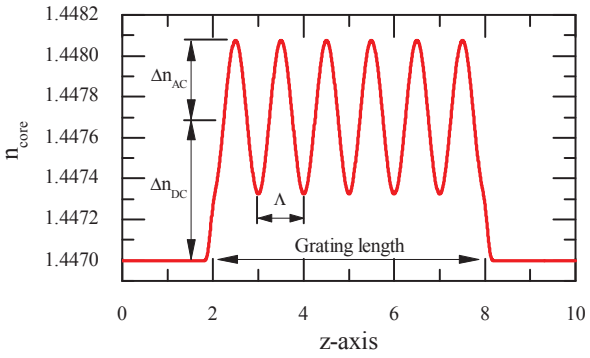

Figure 2: Refractive index profile of a FBG.

In a highly birefringent fibre, the effective refractive index can be divided into two fractions related to the fast $(n_{eff,fast})$ and slow $(n_{eff,slow})$ optical axis of the fibre. The birefringence (B) of a fibre can be described as the difference of both refractive indices,

$$B = n_{eff,slow} - n_{eff,fast} = \lambda / L_B, \tag{3}$$

as well as the wavelength λ of the propagating light divided by the beat-length L_B. The beat-length is the length over which a 2π phase retardation is introduced between the two polarisation modes. Most optical waves propagating along the fibre are nearly unaffected by a fibre Bragg grating, but for a certain wavelength the periodic structure acts as a reflector with a pronounced reflectivity. This so-called Bragg-wavelength λ_B, satisfies in a HiBi-fibre the conditions[7],

$$\begin{aligned} \lambda_{B,slow} &= 2 \cdot n_{eff,slow} \cdot \Lambda, \\ \lambda_{B,fast} &= 2 \cdot n_{eff,fast} \cdot \Lambda, \end{aligned} \tag{4}$$

where $n_{eff,slow}$, $n_{eff,fast}$ are the effective refractive indices of a HiBi-fibre at the location of the grating. The separation of the Bragg reflection peaks related to the slow and fast optical axis can be described as,

$$\Delta\lambda_{f,s} = \lambda_{B,slow} - \lambda_{B,fast} = 2 \cdot B \cdot \Lambda. \tag{5}$$

As shown in Eq. (2), the inscription process leads to an increase of the effective refractive index. Therefore, the measured Bragg-wavelength as function of the UV dose has to be extrapolated to zero UV dose $(d = 0)$, giving to the so-called design wavelength λ_D[8],

$$\lambda_D = n_{eff}(d = 0) \cdot \Lambda_{\mathrm{PM}}. \tag{6}$$

Additionally, a slight offset of the design wavelength has to be considered, due to a certain amount of strain (ε) applied to the fibre during the inscription process. The mean refractive index of the pristine fibre at zero strain and zero dose can be obtained by[8],

$$n_{eff}(\varepsilon = 0, d = 0) = \frac{n_{eff}(d=0)}{[1 - p_e \cdot \varepsilon]} = \frac{\lambda_D / \Lambda_{\mathrm{PM}}}{[1 - p_e \cdot \varepsilon]}, \tag{7}$$

where p_e is the effective photo-elastic coefficient of an optical fibre.

Experiment

As a first step towards the development of FBGS for highly accurate measurements, we investigated the inscription process of FBGs into polarisation maintaining fibres (PMF). To achieve a significant separation of the Bragg reflection peaks it is necessary to use fibres with very high-birefringence, so-called HiBi-fibres. We inscribed FBGs in high-birefringent optical fibres employing the so-called phase mask technique[6].

Our intention in this study was to compare the Bragg-peak separation, i.e. the magnitude of the birefringence, and the effective refractive indices for both the fast and slow optical axis of fibres which differ in material composition and cladding diameter. We choose HiBi-fibres with Panda type stress applying parts (PM1550-HP, Nufern; PM15-U25, Corning; PSPM-60, Coreactive; PSPM-980, Nufern) and Bow-Tie type stress applying parts (HB1500G, Fibercore). The main parameters specified by the manufacturer of the fibres used in this investigation are compiled in Table 1.

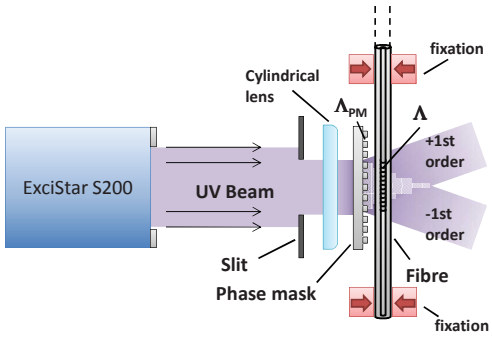

Figure 3: Phase mask inscription schematic.

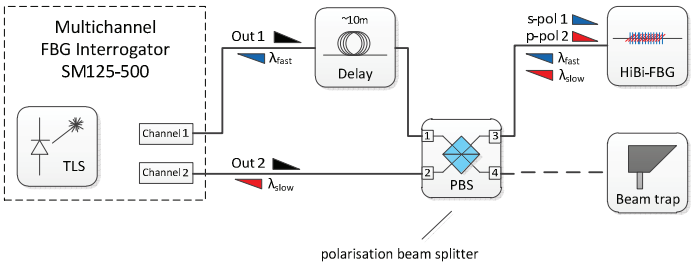

Figure 4: Schematic of the experimental setup.

For FBG generation, we used our in-house FBG inscription facility, which is based on an Excimer laser (ExciStar S200, TUI/Coherent) and a phase mask (O/E Land). Before exposure, the fibre coatings were removed with a standard stripping tool. When the optical fibre was installed in the FBG inscription device, it was fixed with a certain stress between two fibre clamps. The output power of the Excimer laser was focused by a cylindrical lens and the optical fibre was placed close to the focus line of the laser beam within the interference pattern that was created by the phase mask (see Figure 3). The average laser power was measured before and after each inscription process, using a power meter (FieldMaster, Coherent). Dividing the average power by the pulse repetition frequency (PRF = 100 1/s), gives an estimate of the mean UV pulse energy.

The reflection spectra of the fast and slow optical axis of the fibre-Bragg-grating were observed simultaneously during the inscription process with a multichannel FBG interrogator (SM125-500, Micron Optics) in combination with a polarising beam splitter (PBS), see Figure 4. The output light of the FBG interrogator used in this study was measured with a polarisation Analyser (N7788B, Agilent) and found to be partially polarised (DOP ~ 0.3). The principle of this measurement setup is to split the light from the interrogator into s- and p-polarised light. The s-polarised light of channel 1 is reflected at the PBS and couples into the fast optical axis of the HiBi-fibre (depending on the orientation of the fibre). The p-polarised light of channel 1, transmitted through the polarising beam splitter is absorbed in an optical trap. The s-polarised light reflected at the HiBi-FBG is again coupled back into channel 1 of the FBG interrogator. The spectral shape function obtained with channel 1 corresponds to the light reflected at the HiBi-FBG, propagating in the fast optical axis of the HiBi-fibre. Correspondingly, the p-polarised light of channel 2 is coupled by the PBS into the slow axis of the HiBi-fibre. The spectra obtained with channel 2 are equal to the light reflected at the FBG, propagating in the slow optical axis. Additionally, a delay line was attached between the PBS and channel 1 to avoid interferences within the optical bench due to a coherence length of ~1m of the SM125-500 light source. Due to the measurement setup, the polarised fraction of the light may only affect a small change in the Bragg peak amplitude but no change in its wavelength λ_B.

Figure 5 illustrates the peak separation of FBGs inscribed into low-birefringent (GF1B), medium-birefringent (PSPM-60) and high-birefringent (HB1500G) fibres. The spectra corresponding the fast and slow optical axis were obtained with the above described measurement setup. The peaks of the spectral

Table 1: Optical fibres investigated in the present study.

Fiber type / Manufacturer	Diameters: mode field / cladding / coating [µm]	Type of stress applying part	beatlength / at reference wavelength
PM1550-HP / Nufern	10.5 / 125 / 245	Panda	≤5.0mm / 1550nm
PM15-U25 / Corning	10.5 / 125 / 245	Panda	3.0 – 5.0mm / 1550nm
PSPM-60 / Coractive	5.5 / 125/ 250	Panda	≤5.0mm / 1550nm
PSPM-980 / Nufern	6.6 / 125 / 245	Panda	≤3.3mm / 980nm (~5.2mm / 1550)
HB1500G / Fibercore	7.9 / 80 / 170	Bow Tie	≤1.5mm / 630nm (~3.7mm / 1550)

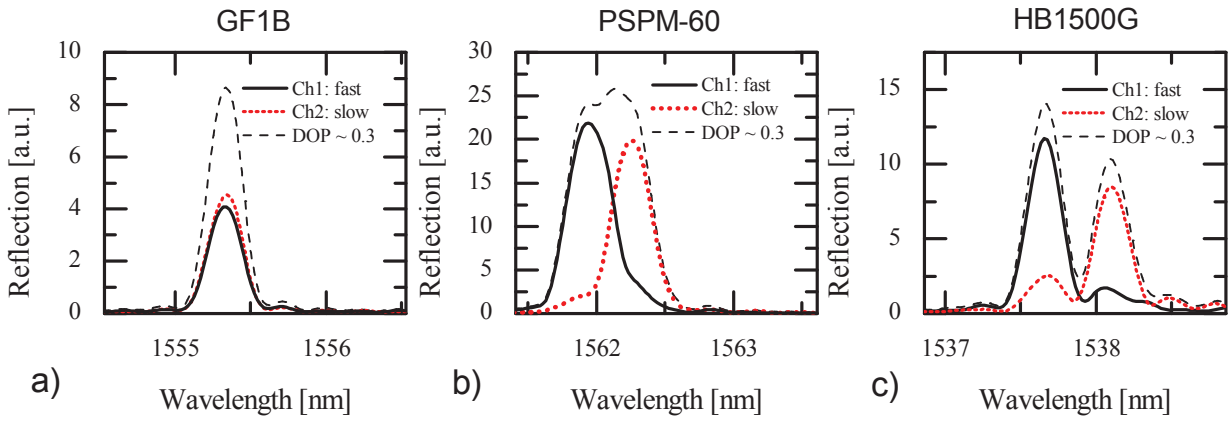

Figure 5: Spectral shape functions of fibre-Bragg-gratings inscribed into a) low-, b) medium-, and c) high-birefringent fibres. The red and black lines indicate the spectral shape function corresponding to the slow and fast optical axis. The dashed black lines show the reflection spectra of the FBGs measured with slightly polarised light (DOP~0.3).

shape functions were well approximated by quadratic functions and the centre wavelengths were determined with high precision. The additional spectra (dashed line), obtained with another channel of the FBG interrogator, illustrate the reflection signal of the FBGs when obtained at a DOP of ~ 0.3. The UV-light dose d [J], to which the fibre was exposed, can be assumed to be proportional to the mean UV pulse energy, multiplied by the number of pulses.

In Figure 6, the Bragg-wavelengths (λ_B) corresponding to the fast and slow optical axis are plotted as a function of the exposure dose (d). This graph, the so-called FBG inscription curve, shows the typical behaviour of a non-linear increase of λ_B as a function of UV dose d. In order to determine the design wavelength, i.e. to extrapolate the Bragg-wavelength λ_B to its zero UV dose $(d = 0)$, a linear regression calculation was applied to the first 10 data points and the ordinate intersection of the fitted linear function is taken as λ_D, as is shown in the insets of Figure 6. Care was taken that the first data point of the FBG inscription curve was taken at the smallest possible UV dose. At the end of each inscription procedure, the fibre was released from its fixations and the Bragg-wavelengths of the unstressed fibre were measured again. As can be seen in Figure 6, the unstrained fibre showed a significantly lower value and the corresponding wavelength change $\Delta\lambda(\varepsilon) = \lambda_{B,s} - \lambda_{B,u}$ between the final value in strained $(\lambda_{B,s})$ and unstrained $(\lambda_{B,u})$ condition was used to determine the strain ε of the fibre installed in the FBG inscription facility,

$$\varepsilon = \frac{\lambda_{B,s} - \lambda_{B,u}}{\lambda_{B,u}} \cdot \frac{1}{(1 - p_e)} = \frac{\Delta\lambda(\varepsilon)}{\lambda_{B,u}} \cdot \frac{1}{(1 - p_e)} \tag{8}$$

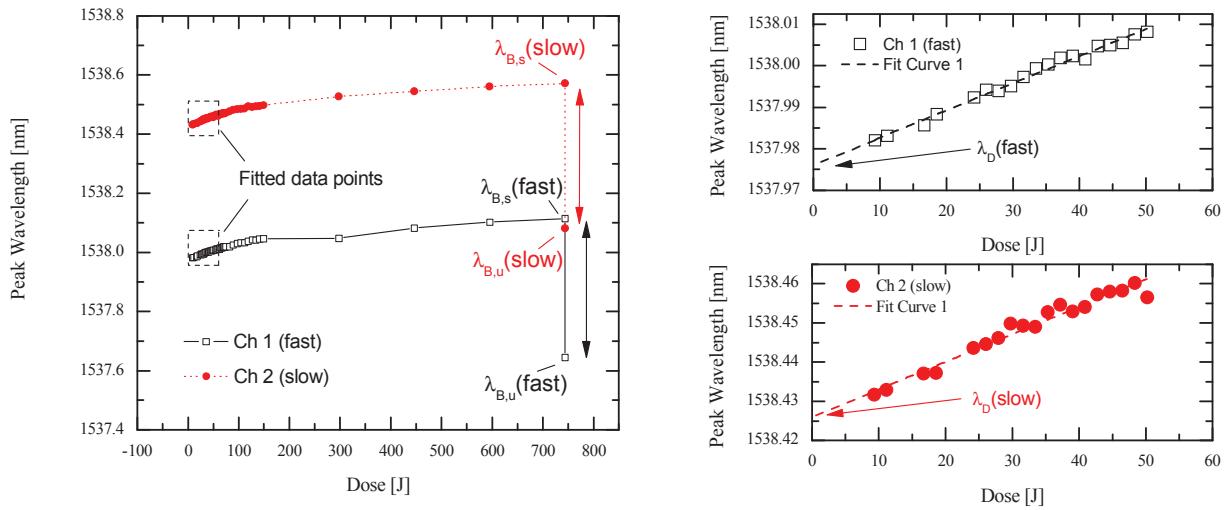

Figure 6: Inscription curve of a fibre Bragg grating into a high birefringent fibre (HB1500G, Fibercore). The two insets show the extrapolation of the Bragg wavelength to its zero UV-Dose.

Results

The FBG interrogator used in this study has a build-in continuous NIST traceable wavelength reference for internal calibration. The wavelength accuracy of the FBG interrogator is specified to be ±1pm in the range of 1510nm - 1590nm. The time lag of the light waves of channel one propagating forwards and backwards through ~10m delay line equals a wavelength shift of ~0,02pm and may therefore be neglected. The uncertainty of the design wavelength λ_D was estimated to be $\sigma_{\lambda_D} = 20pm$, which is mainly attributed to the fact, that a nonlinear relationship was approximated by a linear function. The wavelength uncertainty of the FBG interrogator may therefore be neglected compared to the linear extrapolation of the inscription curve. The effective refractive indices corresponding to the fast and slow optical axis were calculated according to Eq. (7). The effective photo-elastic coefficient was approximated to be $p_e = 0.205$ with an estimated uncertainty of 10% for all fibres[9] and both polarisation modes. The phase masks which were used for the inscription of FBG have a manufacturer specified accuracy of the grating period Λ_{PM} of $\sigma_{\Lambda_{PM}} \leq 0.1nm$. This specified accuracy is the dominant uncertainty in the determination of n_{eff}. Additional uncertainties by the tilt of the optical fibre relative to the phase mask and temperature drifts during the measurement can be neglected relative to the uncertainty of the phase masks pitch[8]. The total uncertainty in determining n_{eff} at the corresponding wavelengths can be estimated to be $\sigma_{\mathrm{n}_{eff}}/\mathrm{n}_{eff} \cong 1 \cdot 10^{-4}$. The refractive indices of all fibres with their total uncertainties are presented in Table [2] and are shown in Figure 8. The peak separation $\Delta\lambda_{f,s}$ and the beat lengths L_B were calculated from the design wavelengths λ_D according to Eq. (3 & 5) and are shown in Figure 9. The beat length, i.e. peak separation, was monitored during the inscription process of several HiBi-FBGs as depicted in Figure 7. The UV induced beat length change $\Delta\mathrm{L}_B = \mathrm{L}_{B,D} - \mathrm{L}_{B,inscribed}$ varied in amplitude and sign for each inscription process.

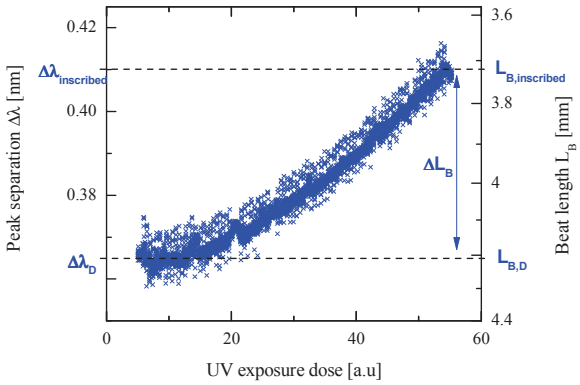

Figure 7: Peak separation / beat length of a PM1550-HP fibre as function of UV-dose.

Conclusion

The refractive indices of the fast and slow optical axis of several types of high birefringent fibres were determined at $\lambda \sim 1540nm$. Within the precision of the measurement, significant differences of the effective refractive indices were found (e.g. $n_{eff,fast}{}^{PM15-U25} = 1.44754 \pm 0.00014$, $n_{eff,fast}{}^{PSPM-60} = 1.45424 \pm 0.00014$). The high birefringence necessary for a significant peak separation $(\Delta\lambda_{f,s} \geq 0.3nm)$ were fulfilled by most of the fibres used in this study. The magnitudes of the beat length, i.e. birefringence, determined for all fibres in this study, are in good agreement with the beat lengths specified by the manufacturer (see Table 1 & 2). For most HiBi-FBGs in this study, a reduction of the beat length was observed during the inscription process. Further investigations of this effect with a larger variety of fibres and well defined azimuthally orientation are needed to clarify whether this behaviour is related to the internal structure or not.

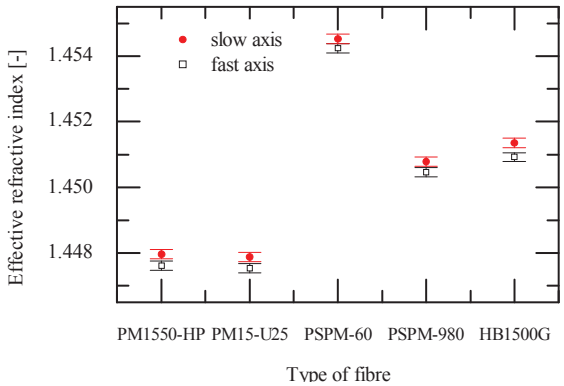

Figure 8: Effective refractive indices with their total uncertainties.

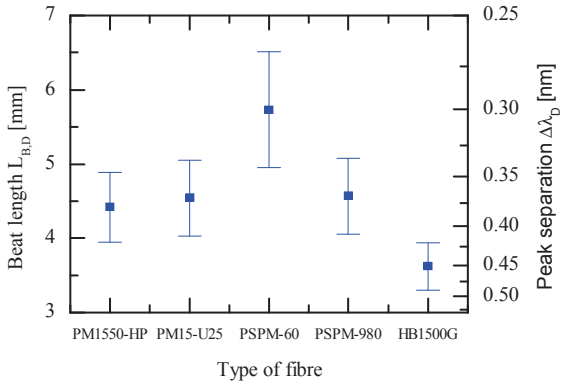

Figure 9: Beat lengths with their total uncertainties.

Table 2: Summary of the significant parameters determined for all fibres in this study.

Fiber Type	Design wavelength λ_D(f) / λ_D(s) [nm]	Strain induced wavelength change $\Delta\lambda$(f) / $\Delta\lambda$(s) [nm]	Effective refractive index n_{eff}(f) / n_{eff}(s)	Peak separation $\Delta\lambda_{f,s}$ [nm] / Beat length L_B [mm]
PM1550-HP	1544.486 ± 0.020 1544.859 ± 0.020	0.219 ± 0.002 0.222 ± 0.002	1.44761 ± 0.00014 1.44796 ± 0.00014	0.373 ± 0.040 4.42 ± 0.51
PM15-U25	1534.395 ± 0.020 1534.754 ± 0.020	0.231 ± 0.002 0.233 ± 0.002	1.44754 ± 0.00014 1.44788 ± 0.00014	0.358 ± 0.040 4.54 ± 0.51
PSPM-60	1561.936 ± 0.020 1562.229 ± 0.020	0.236 ± 0.002 0.268 ± 0.002	1.45424 ± 0.00014 1.45452 ± 0.00014	0.293 ± 0.040 5.73 ± 0.78
PSPM-980	1542.976 ± 0.020 1543.335 ± 0.020	0.077 ± 0.002 0.078 ± 0.002	1.45046 ± 0.00014 1.45079 ± 0.00014	0.359 ± 0.040 4.57 ± 0.51
HB1500G	1537.976 ± 0.020 1538.426 ± 0.020	0.469 ± 0.002 0.491 ± 0.002	1.45092 ± 0.00014 1.45135 ± 0.00014	0.450 ± 0.040 3.62 ± 0.32

Acknowledgements

The authors would like to thank A. Gillooly (Fibercore, Southampton, United Kingdom) for providing us with high birefringent gyro fibres. This work was supported by the Bavarian Minister of Research and Technology.

References

[1] K. O. Hill*, et al.*, "Photosensitivity in optical fiber waveguides: Application to reflection filter fabrication," *Applied Physics Letters,* vol. 32, pp. 647-649, 1978.

[2] M. S. Müller*, et al.*, "Fiber Bragg Grating-Based Force-Torque Sensor with Six Degrees of Freedom," *International Journal of Optomechatronics,* vol. 3, pp. 201 - 214, 2009.

[3] K. O. Hill*, et al.*, "Birefringent photosensitivity in monomode optical fibre: application to external writing of rocking filters," *Electronics Letters,* vol. 27, pp. 1548-1550, 1991.

[4] E. Collett, *Polarized light in fibre optics*, 2003.

[5] A. Othonos and K. Kalli, *Fiber Bragg gratings : fundamentals and applications in telecommunications and sensing*. Boston, Mass.: Artech House, 1999.

[6] K. O. Hill*, et al.*, "Bragg gratings fabricated in monomode photosensitive optical fiber by UV exposure through a phase mask," *Applied Physics Letters,* vol. 62, pp. 1035-1037, 1993.

[7] R. Kashyap, *Fiber Bragg gratings*, 2nd ed. Burlington, MA: Academic Press, 2010.

[8] F. Jülich and J. Roths, "Determination of the Effective Refractive Index of Various Single Mode Fibres for Fibre Bragg Grating Sensor Applications," in *proc. Opto 2009*, Nuernberg, 2009.

[9] J. Roths and F. Jülich, "Determination of strain sensitivity of free fiber Bragg gratings," in *proc. SPIE, vol. 7003, p. 700308*, 2008.